

## Article

# Reconstruction of Spatial–Temporal Changes in Cropland Cover from 1650 to 1980 in Taiyuan City

Meng Li <sup>1</sup>, Xueqiong Wei <sup>1,\*</sup> and Beibei Li <sup>2</sup>

<sup>1</sup> School of Geographical Sciences, Nanjing University of Information Science and Technology, Nanjing 210044, China

<sup>2</sup> Research Institute for History of Science and Technology, Nanjing University of Information Science and Technology, Nanjing 210044, China

\* Correspondence: xueqiong.wei@nuist.edu.cn

**Abstract:** As a crucial component of studies on land use and cover change (LUCC), the reconstruction of historical cropland cover is important for assessing human impact on the environment. This study collects cropland records of each county in Taiyuan City based on historical documents, agricultural statistics, and survey data such as the *Gazetteers*, *Agriculture and Commercial Statistics Table* and *Datasets of Land and Resources of China*. The cropland area at the county level from 1650 to 1980 is determined by revising, correcting, and extrapolating the obtained historical records. By assessing the driving physiogeographic factors for the distribution of cropland through GeoDetector, we establish a land suitability-based gridded allocation model. The cropland areas at the county level are allocated into 1 km × 1 km grid cells. Our results indicated the following. (1) The total cropland area increased since the Qing Dynasty, reaching its maximum value in 1937, after which it declined due to the impact of urbanization after 1937. (2) In terms of the spatial distribution patterns of cropland, from 1650 to 1980, the cropland was mainly distributed in the Fenhe River Valley Plain, and the cropland expanded from the center to the south after 1952. (3) Comparing the reconstruction results for 1980 with the 1 km resolution satellite-based cropland cover data, differences of most (95.77%) grids are between −20% and +20%, comparing the HYDE3.2 dataset with our results. The HYDE3.2 dataset is distinctly lower than our datasets, and the grids with large differences are mainly in the central and southern parts of the study area, especially in the Qing Dynasty. Our reconstruction could evaluate the accuracy of the global dataset when applied to regional areas and serve as base data in studying historical climate change.



**Citation:** Li, M.; Wei, X.; Li, B.

Reconstruction of Spatial–Temporal Changes in Cropland Cover from 1650 to 1980 in Taiyuan City. *Land*

2024, 13, 36. <https://doi.org/10.3390/land13010036>

Academic Editor: Le Yu

Received: 19 November 2023

Revised: 17 December 2023

Accepted: 26 December 2023

Published: 28 December 2023



**Copyright:** © 2023 by the authors. Licensee MDPI, Basel, Switzerland. This article is an open access article distributed under the terms and conditions of the Creative Commons Attribution (CC BY) license (<https://creativecommons.org/licenses/by/4.0/>).

**Keywords:** historical cropland cover; land suitability; gridded allocation; Taiyuan City

## 1. Introduction

Land cover is the source and sink of material and energy flows that support the Earth system. The land cover caused by human land use inevitably affects global and regional climate and environmental changes by altering biophysical processes and biogeochemical cycles [1–5]. The biogeochemical warming of mean annual global surface air has been shown by observation-based estimation in response to greenhouse gas emissions from anthropogenic land cover change since 1901, while biophysical cooling results from surface albedo and decreased turbulent heat fluxes have been derived from models [6]. Thus, historical land use/cover change (LUCC) forms a crucial research component within numerous international scientific programs focused on global change [1,7]. Changes in land surface patterns influenced by LUCC are one of the focuses of the “Future Earth”, a 10-year program (2014–2023) that amalgamates the four primary scientific programs: World Climate Research Program (WCRP), International Geosphere-Biosphere Program (IGBP), DIVERSITAS, and International Human Dimensions Program on Global Environmental Change (IHDP) [8,9]. The achievement of the researchs goals of the “Future Earth” program requires the support of historical land use data with high spatiotemporal resolution [10–13].

Driven by various global change research programs, four representative global historical LUCC datasets have been developed, HYDE [14–17], SAGE [18], PJ [19] and KK10 [20,21] datasets. The data sources of these datasets are the crop, wood harvest and pasture information from the FAO and some countries. Most of the datasets use land suitability models to allocate cropland areas. Since 1997, the HYDE dataset has been continuously revised and extended. The latest version, HYDE 3.2, provides cropland, pasture, and irrigated areas with a resolution of  $5' \times 5'$ , covering the period from 10,000 BC to 2015 [17]. Based on HYDE, Earth system models (ESMs) have led to a harmonization of land-use scenarios (LUH dataset) [22] and the harmonization of global land use change and management (LUH2 dataset) [23] to simulate the effects of human land use on the carbon-climate system. In addition, HYDE3.2 and LUH2 datasets are combined to create a series of global cropland datasets with a resolution of 1 km from 10,000 BCE to 2100 CE [24]. In addition to global datasets, research focused on reconstructing historical LUCC has produced numerous datasets in many countries [25–29]. Comparing global datasets with land use reconstructions in countries, there are still significant uncertainties in global land use datasets, with underestimation or overestimation occurring in many regions, especially in the comparison of cropland area [30–32]. Therefore, one of the goals of the LandCover6k program is to improve the quality of global-scale historical land use/cover datasets based on more reconstructions at different spatial scales [12,33].

Due to its long agricultural history, China has abundant historical documents that serve as valuable data sources for reconstructing historical cropland changes. Representative studies focus on producing the spatial explicit cropland datasets over the past 300 years using the provincial-level cropland area [34,35]. The latest cropland reconstruction at the country level has extended the period to the past 1000 years [29]. At regional scales, northeast China, north China, and some special river basins are selected as the study area of historical cropland reconstruction. For instance, Ye et al. [36] used a multi-sourced data conversion model and documented data calibration to reconstruct the changes in cropland cover at the county level in northeast China over the past 300 years. Wu et al. [37,38] introduced an allocation model based on the settlement density for historical cropland cover and reconstructed the spatial cropland patterns in farmland areas of Shangjing Dao in northeast China during the Liao Dynasty around 1100AD and in Jilin Province over the past 300 years with a resolution of  $5' \times 5'$ . Wei et al. [39] provided the cropland area datasets at a  $10 \text{ km} \times 10 \text{ km}$  grids scale for seven time points from the late 17th century to 2008 in the North China Plain Area. In the Dongting Plain, the county-level cropland areas during 1750–1985 were reconstructed and allocated into  $0.5' \times 0.5'$  grid cells [40]. Huo et al. [41] built a gridded model for cropland in small-scale mountainous areas and reconstructed cropland patterns with a resolution of 30 m from 1700 to 1978 in the Zhangjiu River Basin. Wang et al. [42] developed a spatially explicit random forest model to allocate the county-level cropland area in the Tuojiang River Basin into  $30 \text{ m} \times 30 \text{ m}$  grid cells during 1911–2010 by combining historical archive data with natural and anthropogenic variables.

However, regional differences in the number of historical materials and affecting factors about the spatial distribution of cropland force more regional reconstructions to improve the accuracy of existing historical land use reconstruction datasets. In the Loess Plateau, a rigorous estimation of biophysical processes and biogeochemical cycle changes affected by anthropogenic land use has been hindered by the paucity of historical cropland data, requiring regional materials as data sources and the most suitable cropland allocation model for the regional scale. This study focuses on Taiyuan City in the Loess Plateau, which is the capital city of Shanxi Province, and a highly cultivated area had already appeared in the Fenhe River Basin in the Sui Dynasty (581–618AD) [43]. Based on historical gazetteers, the survey data, and statistics sources, the county-level cropland areas in nine time points during 1650–1980 are reconstructed. Then, by selecting physiogeographic factors for the study area and using the new cropland gridded allocation algorithm based on land suitability employed by Zhang et al. [44], a cropland cover dataset covering Taiyuan City with a resolution of  $1 \text{ km} \times 1 \text{ km}$  is produced. Moreover, we analyze the key turning

points of changes in cropland areas and the spatial distribution changes of cropland. Our results provide a systematic description land development history in Taiyuan City over the past 300 years. Gridded cropland data also can evaluate the accuracy of the global dataset and serve as the base data for climate or environmental change study.

## 2. Study Area

Located at the eastern end of the Loess Plateau, Taiyuan City ( $111^{\circ}30' \sim 113^{\circ}09' \text{ E}$ ,  $37^{\circ}27' \sim 38^{\circ}25' \text{ N}$ ) is surrounded by mountains in northwest and northeast. The central and southern part of Taiyuan City is the low and flat Fenhe River Valley Plain (Figure 1). The study area has an average annual temperature of 8.1 to 11 °C and a continental warm-temperate monsoon climate with 390 to 423 mm of precipitation on average [45]. Although light and heat resources are enough for crop cultivation, water resources are relatively inadequate. The land area of Taiyuan is 6988 km<sup>2</sup>, of which cropland, garden land, grassland, forest land, and construction land accounted for 16.68%, 2.60%, 24.10%, 39.79%, and 9.25%, respectively, in 2020 (<https://www.taiyuan.gov.cn/> (accessed on 8 August 2023)).

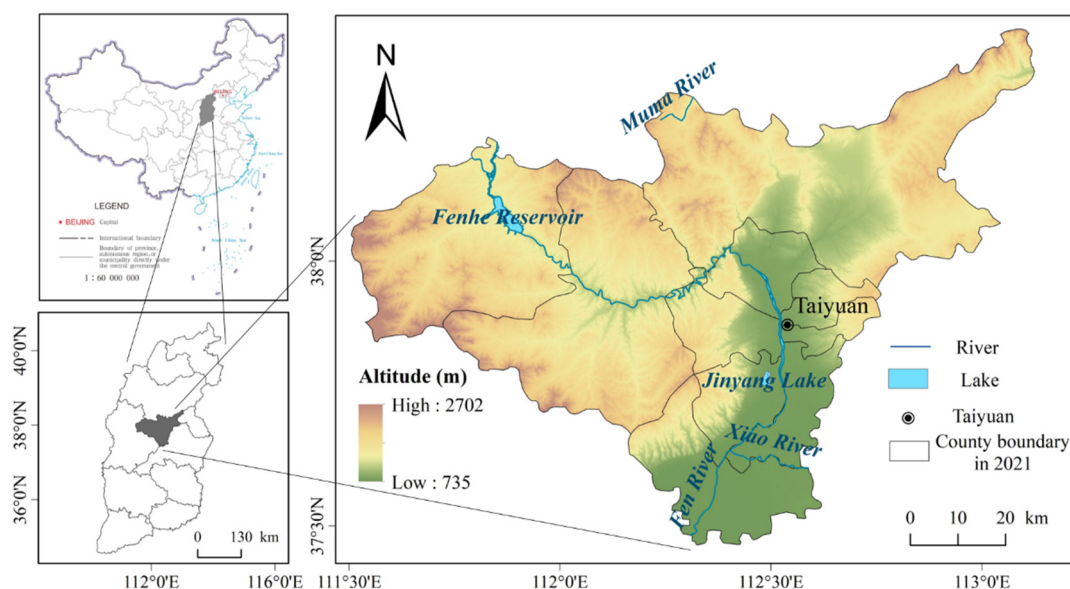


**Figure 1.** Location of the study area.

Taiyuan City serves as the economic, political, and cultural center of Shanxi Province. Its agricultural history can be traced back to the late Paleolithic period, during which domesticated crops like corn and millet were cultivated on both sides of the Fenhe River. From the Tang Dynasty to the Yuan Dynasty (618–1368 AD), Taiyuan Prefecture had always been the agricultural center of Shanxi Province and was constantly developing. The Tang and Northern Song Dynasties, the early and middle Ming Dynasty and the middle Qing Dynasty are three peak periods of rice production [46]. Due to the droughts in the late Qing Dynasty, the planting mode in the Taiyuan Basin shifted from paddy farming to dryland farming, and the planting area of fruits and vegetables expanded. The rapid growth of population led to an increase in cropland area, but food shortages were still unavoidable [47].

The historical administrative division of Taiyuan City has changed many times. During the reign of Shunzhi (1644–1661 AD) and Kangxi (1622–1722 AD) periods in the Qing Dynasty, the administrative division of Taiyuan Prefecture was consistent with that of the Ming Dynasty, comprising 5 departments (*Zhou*) and 20 counties (*Xian*). In 1724, Taiyuan Prefecture was comprised of four departments: Pingding, Dai, Baode, and Xin Departments. By the end of the Qing Dynasty, Taiyuan Prefecture governed one department and ten counties [48]. According to the spatial range of Taiyuan City in modern times, only seven

counties including Yangqu, Taiyuan, Xugou, Jiaocheng, Jingle, Yu, and Yuci Counties were covered as the administrative division of Taiyuan City in 1911 (Figure 2a). By 1912, Taiyuan Prefecture was abolished, and Taiyuan City was governed by Yangqu County. In 1921, the government established the Taiyuan Municipal Office, and a modern administrative method was used to divide Taiyuan City [49]. In 1949, Taiyuan City was converted into a provincial municipality, and Yuci County no longer belonged to Taiyuan City (Figure 2b). In 1960, Taiyuan City included the Taiyuan Municipal District as well as Qingxu, Yangqu, Loufan and Gujiao Counties (Figure 2c). In 1997, Taiyuan Municipal District was divided into six districts: Xiaodian, Yingze, Xinghualing, Jiancaoping, Wanbailin, and Jinyuan Districts. Currently, Taiyuan City governs six districts, three counties, and one county-level city (Figure 2d).

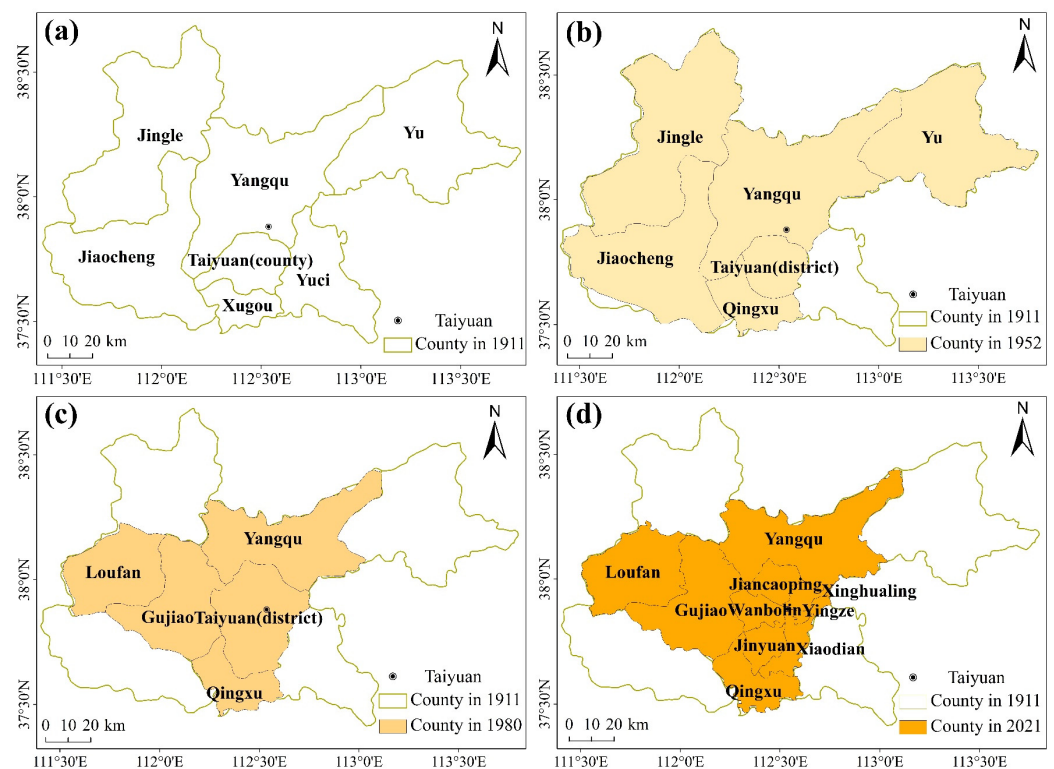


**Figure 2.** Administrative divisions of Taiyuan City in four periods: (a) 1911; (b) 1952; (c) 1980; (d) 2021.

### 3. Data Sources and Methods

#### 3.1. Data Sources

##### 3.1.1. Cropland Data

Cropland area data at the county level are collected from local gazetteers, agricultural survey data, and statistics data in the Republic of China and after 1949. According to the book *A General Catalogue of Gazetteers in China* [50], 37 local gazetteers may provide historical cropland area information in modern Taiyuan City. Based on the National Digital Library of China and the book *Collection of Chinese Gazetteers Shanxi Province* [51], we have collected 16 gazetteers in the Qing Dynasty and the Republic of China, including county, prefectural and provincial gazetteers. The records of tax-paying land data and land tax are an important source of each administrative unit's cropland area data during the Qing Dynasty. We have compiled 62 records regarding the tax-paying land area at the county and prefectural level for Taiyuan City.

The data of records from local gazetteers are too scarce to reflect the change in cropland during the Republic of China, so we add the survey data [52] and the *Agriculture and Commercial Statistics Table* [53] as supplementary data sources. The county-level cropland

area in 1952 is extracted from the book *Compilation of Statistics on Agriculture, Forestry and Water Resources in Shanxi Province, Prewar-1956* [54]. The cropland area in the 1980s are collected from the books of *Summary of Rural Economic Statistics by County in China (1980–1987)* published by the National Bureau of Statistics [55], and *Datasets of Land and Resources of China* published by the Committee for Integrated Survey of Natural Resources in the Chinese Academy of Sciences and State Planning Commission [56].

The population data is obtained from the book *History of Chinese Population · Volume 5* [57], *History of Chinese Population · Volume 5* [58], and *Compilation of Demographic Historical Materials of the Republic of China* [59].

### 3.1.2. Data Used in the Cropland Gridded Allocation Model

Data used in the cropland gridded allocation model include physiogeographic factors and modern gridded cropland data (Table 1). A total of 12 physiogeographic factors, including altitude, slope, the annual mean precipitation and temperature, soil organic carbon density, bulk density, texture, and pH are chosen for analyzing their relationship with the spatial distribution of cropland. Moreover, we select the normalized difference vegetation index (NDVI) [60] to represent the composite factor of vegetation productivity. The modern gridded cropland area data are obtained through the integration of remote sensing data in 1980s, 1995 and 2000 [61].

**Table 1.** Physiogeographic data used in this study.

Class	Data	Resolution	Unit	Description and Source
Topography	Altitude	1 km × 1 km	m	From SRTM V4.1 data through resampling ( <a href="https://www.resdc.cn/data.aspx?DATAID=123">https://www.resdc.cn/data.aspx?DATAID=123</a> ) (accessed on 19 April 2023))
	Slope	1 km × 1 km	m	
Climate	Annual Mean Temperature	30" × 30"	°C	Multi-year average from 1970–2000 ( <a href="https://www.worldclim.org/data/index.html">https://www.worldclim.org/data/index.html</a> ) (accessed on 18 April 2023))
	Annual Mean Precipitation	30" × 30"	mm	
Soil	Soil Bulk Density	250 m × 250 m	kg/m <sup>3</sup>	Data area obtained from the soil tillage layer at a depth of 15–30 cm ( <a href="https://soilgrids.org">https://soilgrids.org</a> ) (accessed on 18 April 2023))
	Soil Organic Carbon Density	250 m × 250 m	kg/m <sup>3</sup>	
	Coarse Fragments Content	250 m × 250 m	%	
	Sand content	250 m × 250 m	%	
	Clay Content	250 m × 250 m	%	
	Silt Content	250 m × 250 m	%	
	pH	250 m × 250 m	--	
Vegetation	NDVI	1 km × 1 km	--	NDVI in 2000 ( <a href="https://www.resdc.cn/DOI/DOI.aspx?DOIID=49">https://www.resdc.cn/DOI/DOI.aspx?DOIID=49</a> ) (accessed on 19 April 2023))
Cropland	Modern Gridded Cropland Data	1 km × 1 km	%	Integration of remote sensing data in 1980s, 1995 and 2000 ( <a href="https://www.resdc.cn/DOI/DOI.aspx?DOIID=54">https://www.resdc.cn/DOI/DOI.aspx?DOIID=54</a> ) (accessed on 19 April 2023))

The vector map of the county-level administrative divisions in 1911 is downloaded from the Yugong website (<http://yugong.fudan.edu.cn/>) (accessed on 1 January 2023)). The vector map of administrative divisions around 1952 is produced based on three administrative division maps from 1949 to 1964 provided by the OSGeo website (<https://www.osgeo.cn/>) (accessed on 1 January 2023)). The administrative base map in 1980 is from the National Earth System Science Data Center (<http://www.geodata.cn/>) (accessed on 1 January 2023)).

### 3.2. Methods

The methodology for reconstructing the historical cropland cover of Taiyuan City includes the following steps. Based on data sourcing from historical gazetteers, agricultural survey data, and statistics from the Qing Dynasty to 1980 and processes of calibration, correction, and extrapolation, we obtain the historical county-level cropland areas in Taiyuan City. Then, driving factors affecting the cropland's spatial pattern are selected from 12 physiogeographic factors using the GeoDetector tool. Lastly, we construct a cropland gridded allocation model and allocate the county-level historical cropland area during 1650–1980 into a 1 km × 1 km grid (Figure 3).

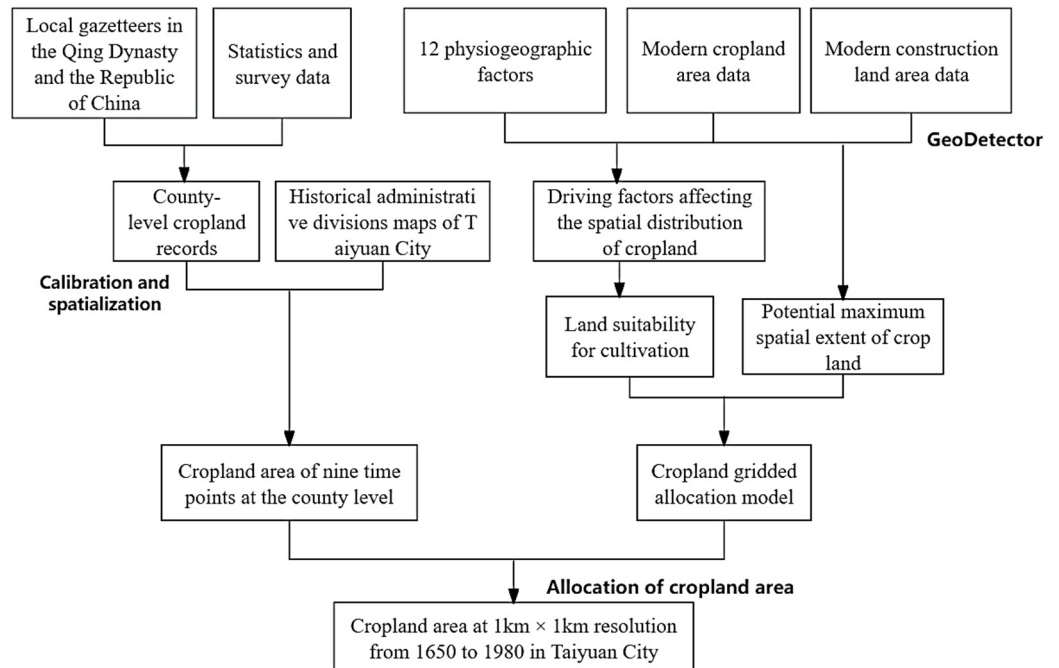


**Figure 3.** Flowchart of the cropland reconstruction.

#### 3.2.1. Collection of the Registered Cropland Data

Our county-level cropland area in the Qing Dynasty is extracted by analyzing the registered tax-paying land data from gazetteers. The government classified the land into different types for taxation, resulting in varying land taxes per unit of tax-paying land. Consequently, even within the same province, recording methods of land taxes vary among different prefectures and counties. In the Qing Dynasty, there were four tax-paying land types recorded in the gazetteers of Taiyuan:

“*Min Tian* (Civilian land)” refers to the tax-paying land cultivated by private civilians;

“*Gengming Tian* (Renamed land)” refers to the land owned by seigniors in the Ming Dynasty. The Manchu government gave these lands to civilians at the beginning of the Qing Dynasty without compensation but collected land taxes as Civilian land;

“*Tun Tian* (Soldier-cultivated land)” refers to the land cultivated by soldiers to supply food for local troops;

“*Xue Tian* (Education land)” refers to the government-owned land and cultivated by civilians who rent it. The land rent is used for teachers’ salaries and subsidies for students.

All the above four types of tax-paying land are cropland and included in the total cropland area of each county. For a certain year, we use the data recorded in the county gazetteer if there are tax-paying land data collected from the county, prefectural and provincial gazetteers. For cases where there is a significant difference in tax-paying land data between two close years, we compare them with survey data and statistics to choose the data that is more in line with the trend of cropland area change. The spatial and

temporal distribution of the registered tax-paying land records at the county level that we used is presented in Figure 4.

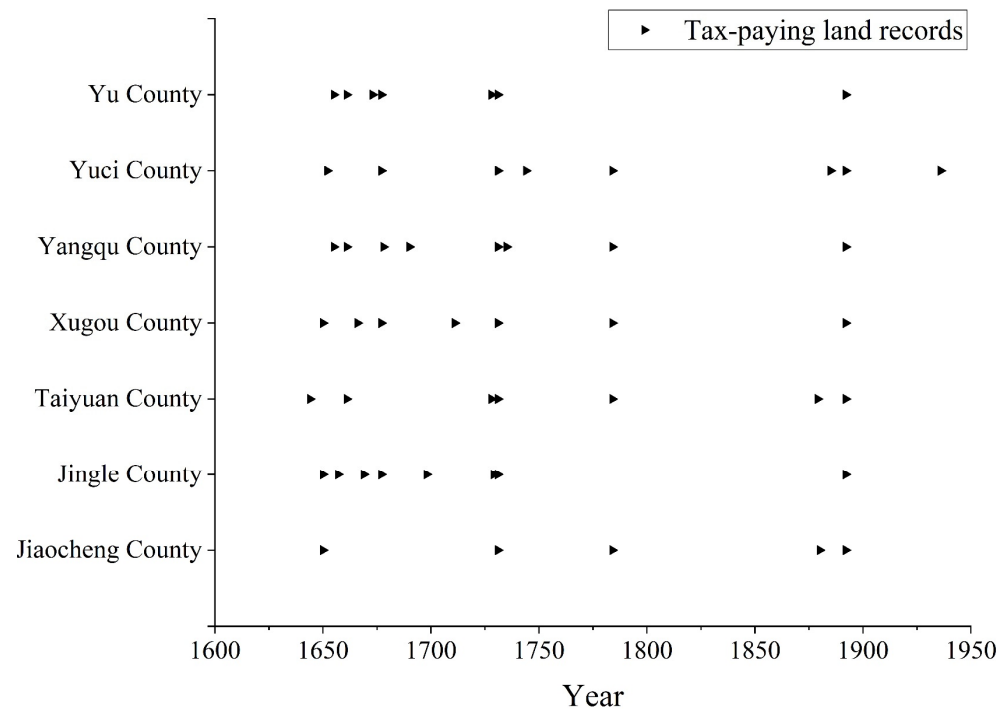


**Figure 4.** Records of tax-paying land at the county level.

The survey data and statistics in the Republic of China and after 1949 quantitatively record the county-level cropland area. Thus, the cropland areas of counties that cover the spatial range of Taiyuan City in modern times are selected directly. Considering the richness of tax-paying land data (Figure 4) and cropland area data for each year, we choose nine time points: 1650, 1680, 1730, 1784, 1892, 1916, 1937, 1952, and 1980.

### 3.2.2. Cropland Data Calibration and Spatialization

In the Ming and Qing dynasties, the tax-paying land data differed significantly from the ‘actual’ cropland area. Moreover, the term “*mu*” employed in registered tax-paying land is not the modern unit of cropland area but rather a unit of taxation, resulting in the registered cropland area being lower than the ‘actual’ cropland area [62]. However, the tax-paying land data still came from the cropland area, so it is possible to obtain data close to the ‘actual’ cropland area by analyzing and calibrating the records of tax-paying land data in gazetteers.

According to historical gazetteers, a discount of *mu* existed in the land registration system of Jiaocheng, Jingle, Yu, Xugou, and Yangqu counties during the Qing Dynasty but not in Taiyuan and Yuci counties. Furthermore, a comparison with modern statistics demonstrated that the registered cropland areas from gazetteers in Xugou and Yangqu counties are reasonable, and we infer that the discount rate of *mu* in these two counties is 1. There is no record about the discount rates of *mu* for Jiaocheng, Jingle, and Yu counties in local gazetteers. Three proofs lead us to the conclusion that the discount rates of *mu* for Jiaocheng, Jingle, and Yu counties are 1.40, 4.42, and 1.58, respectively (Table 2). (1) During the Qing Dynasty, the reconstruction of cropland area changes in northern Shanxi [63]. (2) We compare the registered tax-paying land data with statistics and survey cropland areas during the Republic of China. (3) There is a relatively stable cropland area change trend during 1916–1937 in the Republic of China in Shanxi Province [64]. Subsequently, we calibrate the registered tax-paying cropland area from gazetteers in the Qing Dynasty and cropland area from statistics in the Republic of China for Jiaocheng, Jingle, and Yu

counties based on the discount rates of *mu*. Notably, the cropland area from statistics for Taiyuan City in 1916 are far smaller than that from the survey data in 1937, whereas the reverse is observed for the corresponding two years in Xugou County. The total cropland area of Taiyuan and Xugou counties changed little from 1916 to 1937, but the change in administrative divisions [49] brought a notable increase in cropland area of Taiyuan County but a decrease of Xugou County. Thus, the cropland areas of Taiyuan and Xugou counties in 1916 are estimated based on their contrast in 1937.

**Table 2.** Comparison of cropland areas from survey data and statistics in the Republic of China (unit: km<sup>2</sup>).

County	Cropland Area from Statistics in 1916 (A)	Survey Cropland Area in 1937 (B)	Discount Rate of <i>mu</i> (B/A)
Jiaocheng	156.71	219	1.40
Jingle	134.11	593	4.42
Yu	185.05	293	1.58

Based on the study in the North China Plain Area [65], using 1.2 and 0.9 as the calibration coefficients, we validate the cropland area affected by unregistered land during the Qing Dynasty and exaggeration factors before the Qianlong reign (before 1736).

All counties in Taiyuan City used Qing *mu* (the official unit of land area in the Qing Dynasty). We convert Qing *mu* to square kilometer (km<sup>2</sup>) using the equation: 1 official Qing *mu* = 0.9216 Modern *mu* (a unit of area in modern times) = 0.9216/1500 square kilometer (km<sup>2</sup>). The characteristics of cropland area from statistics during the Republic of China differed from those in the Qing Dynasty. The unit of cropland area from official statistics changed from the Qing *mu* used during the Qing Dynasty to the Modern *mu*. Therefore, we convert units of cropland area from statistics and survey data during the Republic of China from Modern *mu* to square kilometer (km<sup>2</sup>).

The county-level cropland areas from statistics and survey data in 2009 and 2016 are also collected. By comparison, it is found that the cropland area at the county level in Taiyuan City from survey data is 1.4 times higher than that from the statistics after 2000. In the 1980s, there were no differences between the survey data and the statistics, which reflected that the county-level cropland area in Taiyuan City from the survey data was directly derived from the statistics. We improve the cropland area from statistics in 1980 to be in line with the standard of survey data based on the calibration coefficient of 1.4.

Due to frequent administrative division changes in Taiyuan City since the Qing Dynasty, county-level administrative division base maps in modern times are not directly applicable to the historical cropland area. Since the county-level administrative division remained relatively stable from the Qing Dynasty to the Republic of China [48,49], the administrative vector map in 1911 is employed as the base map for the seven time points of cropland data from 1650 to 1937. The base maps for the cropland area data in 1952 and the 1980s were the administrative division maps from 1950 and 1980. After that, the county-level cropland area for each time point is shown on maps.

### 3.2.3. Cropland Area Allocation

#### (1) Selection of driving factors

GeoDetector (<http://www.geodetector.org/> (accessed on 8 August 2023)) is used for analyzing the relationship between modern cropland area and physiogeographic factors, aiming to identify driving factors in the spatial pattern of cropland. As a statistical method, GeoDetector is widely used to detect spatial stratified heterogeneity and reveal the driving factors behind it, which is based on a hypothesis: The spatial distributions of both variables should be similar when an independent variable significantly affects a dependent variable. GeoDetector is composed of four detectors: interaction detector, factor detector, risk detector, and ecological detector. The purpose of the interaction detector is

to determine whether a response variable  $Y$  is influenced interactively by the risk factors  $X_1$  and  $X_2$  (and more  $X$ , if applicable). The purpose of the factor detector is to identify the spatial heterogeneity of  $Y$  and assess the degree to which a particular factor  $X$  accounts for that heterogeneity [66]. The spatial distribution of cropland and physiogeographic factors such as climate, topography, and soil have heterogeneity. Identifying physiogeographic factors with high spatial similarity to cropland is crucial for building a cropland gridded allocation model.

We adjust the spatial resolution of modern cropland area data and 12 physiogeographic factors to  $1 \text{ km} \times 1 \text{ km}$ . The correlations between 12 physiogeographic factors and the modern cropland area data, excluding values of 0, are detected by using interaction detector and factor detector in GeoDetector. The interaction detector reveals that all factors are independent. Factor detector ranks the influence of affecting factors on the spatial distribution of cropland by  $q$  statistic value as follows (Table 3): ALT (0.44) > AMT (0.42) > SBD (0.40) > SOCD (0.37) > SLO (0.36) > PH (0.30). All factors undergo a  $t$ -test with a 0.05 confidence level.

**Table 3.** The detection of physiogeographic factors.

Factors	Altitude	Annual Mean Temperature	Soil Bulk Density	Soil Organic Carbon Density	Slope	pH
Abbreviation	ALT	AMT	SBD	SOCD	SLO	PH
$q$ statistic	0.44	0.42	0.40	0.37	0.36	0.30
$p$ value	0.000	0.000	0.000	0.000	0.000	0.000
Factors	Coarse Fragments Content	Clay Content	Sand Content	Annual Mean Precipitation	Silt Content	NDVI
Abbreviation	CFC	CLC	SAC	AMP	SIC	NDVI
$q$ statistic	0.29	0.26	0.17	0.12	0.05	0.01
$p$ value	0.000	0.000	0.000	0.000	0.000	0.000

We select factors with a  $q$  statistic value more than 0.3. Furthermore, Spearman's correlation analysis ( $p = 0.001$ ) is performed between modern cropland area data, and the six selected physiogeographic factors and the ranking of correlation coefficients is as follows: SOCD ( $-0.588$ ), ALT ( $-0.586$ ), AMT ( $0.576$ ), SLO ( $-0.522$ ), SBD ( $0.425$ ) and PH ( $0.384$ ). To avoid multicollinearity, ALT, AMT, SOCD and SLO are chosen as factors for building the land suitability model.

## (2) Calculation of land suitability for cultivation

Within the administrative boundaries at the county level of each time point, four factors are standardized. For factor (AMT) that has a positive correlation with the cropland area fraction, we use Formula (1) [67], and for factors (ALT, SOCD and SLO) that have a negative correlation with the cropland area fraction, we use Formula (2) [68]:

$$k_{i\text{MaxNorm}} = \frac{k_i - k_{i\text{min}}}{x_{i\text{max}} - x_{i\text{min}}} \quad (1)$$

$$k_{i\text{MinNorm}} = \frac{k_{i\text{max}} - k_i}{k_{i\text{max}} - k_{i\text{min}}} \quad (2)$$

where  $k_i$  is the value of a factor in grid  $i$ ;  $k_{i\text{max}}$  ( $k_{i\text{min}}$ ) is the maximum (minimum) value of the factor in grid  $i$ ; and  $k_{i\text{MaxNorm}}$  ( $k_{i\text{MinNorm}}$ ) is the maximum (minimum) normalized value of the factor in grid  $i$ .

To avoid the exponential scaling effect and oversaturated allocation of cropland caused by a simple multiplication of all factors in a gridded allocation algorithm, the approach

provided by Zhang et al. [44] is used to calculate the land suitability (the interval is 0–1) as Formula (3):

$$Suit_i = \sqrt[4]{ALT_i \times AMT_i \times SOCD_i \times SLO_i} \quad (3)$$

where  $Suit_i$  is the land suitability for cultivation in grid  $i$ ;  $ALT_i$ ,  $AMT_i$ ,  $SOCD_i$ , and  $SLO_i$  represent the value of the normalized ALT, AMT, SOCD, and SLO in grid  $i$ , respectively.

### (3) Allocation of historical cropland area into grids

The satellite-based cropland cover maps in the 1980s, 1995 and 2000 are overlaid as the potential maximum cropland extent for the cropland allocation in the 1980s. Because most of the construction land in modern towns and cities is converted from cropland, the combined area of modern cropland and modern construction land is used as the potential maximum cropland extent for the cropland allocation before the 1980s. The potential maximum extent of cropland derived from the spatial pattern of modern cropland can also represent agricultural activities from ancient times to the present day. The cropland allocation weight  $W_i$  in grid  $i$  is calculated based on Formula (4):

$$W_i = Suit_i \times CF_{max_i} \quad (4)$$

where  $Suit_i$  is the land suitability for cultivation in grid  $i$ ;  $CF_{max_i}$  is the potential maximum cropland extent in grid  $i$ .

It is generally assumed that lands with high land suitability have higher priority for cultivation in history. Therefore, in this study, the cropland area of each county in nine time points within the modern Taiyuan city is allocated to grids with a resolution of 1 km × 1 km based on the value of  $W_i$  of each county from high to low as Formula (5):

$$CropArea_i = CropArea_j \times \frac{W_i}{\sum_{i=1}^i W_i} \quad (5)$$

where  $CropArea_i$  is the cropland area in grid  $i$ ;  $CropArea_j$  is the cropland area in county  $j$ ; and  $W_i$  is the cropland allocation weight of grid  $i$  in county  $j$ .

After allocation, for grids with more than 1 km<sup>2</sup> of cropland area, the extra cropland area is allocated to other grids with less than 1 km<sup>2</sup> of cropland area using Formula (5), and this process is repeated until each grid has less than 1 km<sup>2</sup> of cropland area.

## 4. Results

### 4.1. The Total Cropland Area Changes

Due to frequent changes in the administrative division of Taiyuan City since the Qing Dynasty, we use the administrative division map in 1980 to calculate the total cropland areas in the nine time points. However, the population data are difficult to consider the changes in the administrative division. The changes trend of cropland area from 1650 to 1980 can be divided into four stages (Figure 5):

(1) The cropland area increased continuously from 1650 to 1784, rising from 1346.57 to 1524.48 km<sup>2</sup> with an average annual growth rate of 0.23%. The Manchu conquest at the end of the Ming Dynasty led to depopulation in Shanxi Province, resulting in the abandonment of its cropland. To encourage land recultivation, the Qing government released several agricultural policies during the reign of Shunzhi (1643-1661AD). Concurrently, the garrison implemented land reclamation measures. The government allocated unclaimed wastelands to individuals without land ownership, motivating cultivation activities. During the reign of Kangxi (1661-1722AD), to counter water-related disasters and facilitate agricultural irrigation, the government of Shanxi Province aimed at restoration endeavors involving channels, waterways, embankments, and weirs. These proactive measures not only improved the condition of agricultural production but also facilitated the reclamation of wastelands near rivers. During the Kangxi, Yongzheng, and Qianlong reign periods (1722-1796AD), the achievement of the flourishing age and the policies of reducing agricultural taxes drew

numerous exiles to establish settlements in Shanxi Province. The rapid growth of population in Shanxi Province necessitated the expansion of cropland for production, leading to a gradual increase of cropland area [69].

(2) The cropland area declined slightly from 1784 to 1892 with an average annual growth rate of  $-0.03\%$ . During the mid-period of the Qianlong reign, corruption in government institutions became widespread. Additionally, high land rents, excessive taxation, land annexation and concentration by landlords and bureaucrats, coupled with severe natural disasters in Shanxi Province, increased the burden on farmers and led to the abandonment of cropland. During the reign of Jiaqing (1796-1820AD), numbers of farmers who had been oppressed by the landlords for a long time were involved in revolts. After 1840, to resist foreign invasions and to suppress peasant revolts, the Qing government attempted to alleviate the crisis by imposing additional taxes on cropland taxes paid by farmers. The escalating conflicts between the government and farmers triggered more revolts against the Manchu government, resulting in massive abandonments of cropland [70].

(3) The cropland area increased rapidly from 1892 to 1937, with an average annual growth rate of  $0.46\%$ , reaching its peak at  $2055.68 \text{ km}^2$  in 1937. Due to severe natural disasters [71] and social instability, the rural agriculture development was in a low level during the late Qing Dynasty. To solve the rural production crisis, the government implemented policies to reduce capitation taxes and encourage land reclamation, attracting refugees to return to rural areas for agricultural activities [70]. In the early Republic of China, the government of Shanxi Province believed that agricultural development was the key to the economic progress, and the primary problem of agriculture was water conservation and irrigation. Since 1917, the government had taken a series of measures to construct water conservancy [72]. With sufficient water resources, the land near channels and wells was reclaimed first. In addition, the promotion of economic crops and agricultural technology led to the growth of cropland area in Taiyuan City in the early Republic of China.

(4) The cropland area declined rapidly from 1937 to 1952, with an average annual increase rate of  $-0.98\%$ . Then, it increased after 1952, reaching  $1874.13 \text{ km}^2$  in 1980. During this period, China was involved in the eight years of the Second Sino-Japanese War (1937–1945). China suffered continual attack and was subject to a devastating occupation of much of the nation. In Taiyuan City, Japanese military facilities occupied a large amount of cropland. Due to the impact of the war, farmers were unable and unwilling to farm, resulting in the destruction and abandonment of massive cropland [73]. After 1949, the political economy of agrarian reform “Land to the tiller” was implemented by the government, and approximately one-third of the population in the Jinsui liberated area owned land for cultivation [74]. Combined with the establishment of rural agricultural cooperatives, the land reform was implemented quickly in Shanxi Province. After 1952, the population continued to grow, leading to the comprehensive implementation of agricultural mutual assistance activities, and the promotion of agricultural production technologies promoted the cultivation of more lands and the production of more crops [75].

#### 4.2. Spatial Distribution Patterns of Cropland

The cropland spatial distribution patterns with a resolution of  $1 \text{ km} \times 1 \text{ km}$  at nine time points are shown in Figure 6. Generally, most grids with high cropland fraction are found in the Fenhe River Valley Plain, which is characterized by favorable cultivation conditions like low altitude and fertile soil. There are also a few grids with high cropland fraction in intermountain plains and near rivers. We can find that the cropland was mainly distributed in eastern Taiyuan City over the past 300 years, and the cropland in the northern part was gradually increased until 1937. After 1952, the land of southern Taiyuan City was cultivated intensively.

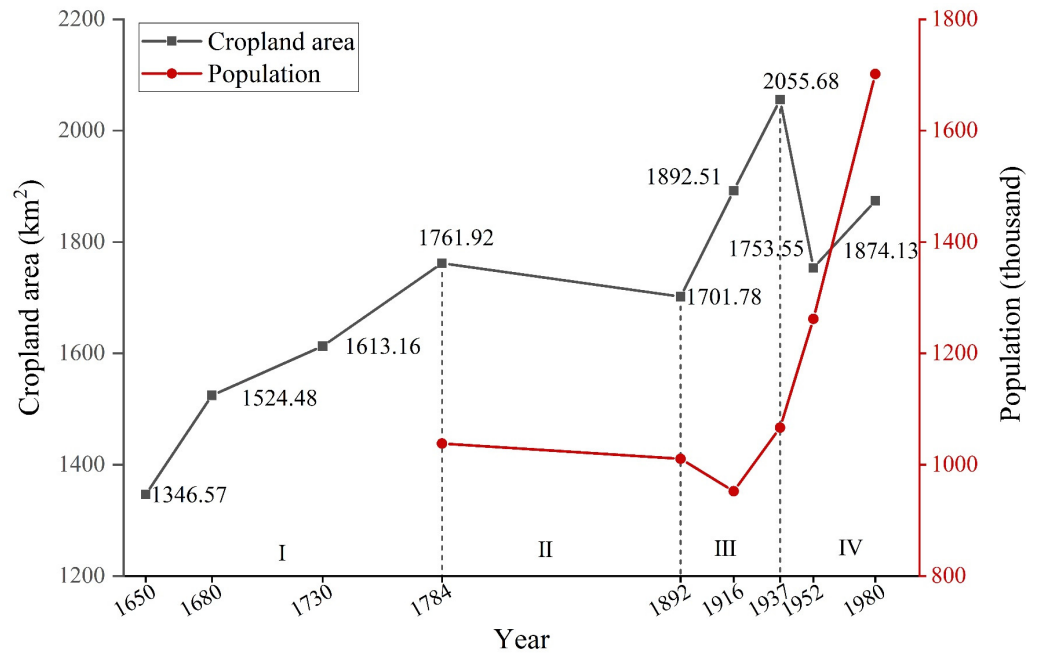


Figure 5. The total cropland area changes in Taiyuan City from 1650 to 1980.

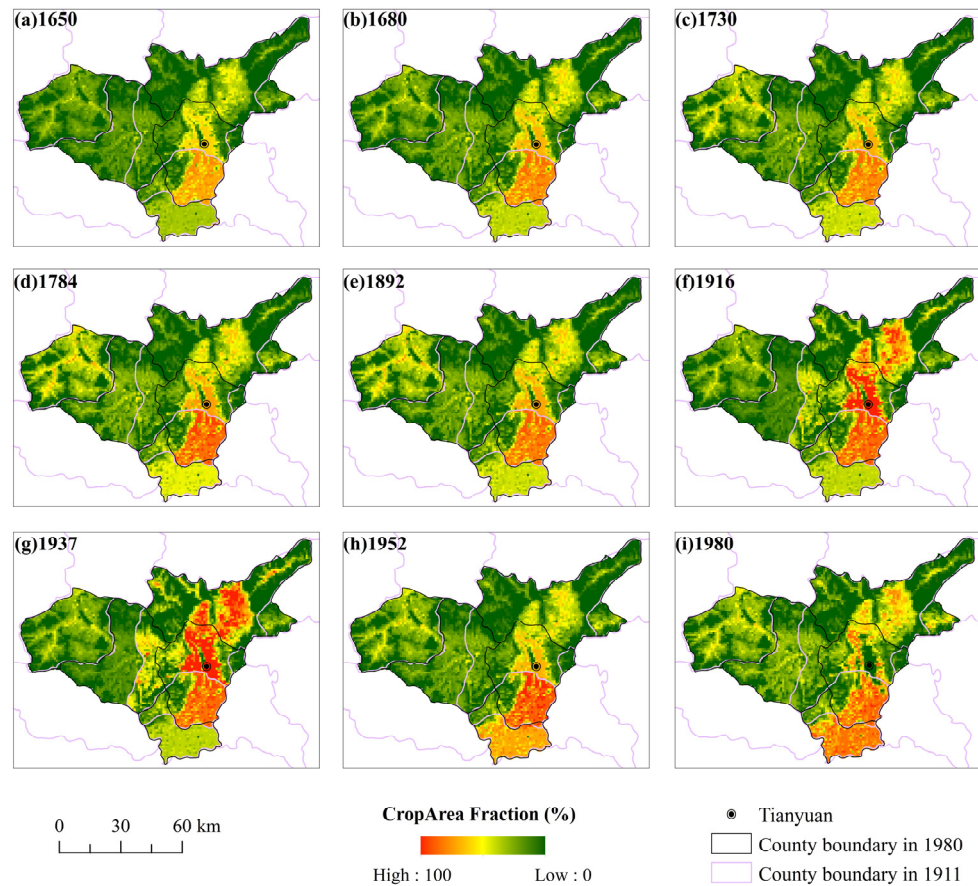


Figure 6. Spatial distribution patterns of cropland from 1650 to 1980 in Taiyuan City.

From 1650 to 1892, the cropland spatial distribution patterns in Taiyuan City remained steady. In 1650, 22.94% of grids had the cropland area fraction of more than 30% (Figure 6a); by 1784, the proportion had risen to 34.77% (Figure 6d). Most grids with high cropland fraction were mainly distributed in the eastern of Taiyuan City with low altitude, including

Taiyuan, Yangqu and Qingxu counties. However, the proportion of grids with cropland area fraction more than 30% declined to 33.86% in 1892 (Figure 6e), which was mainly in central Taiyuan City. Due to the distribution of the Fenhe River, Jian River, Nanchuan River, and Xichuan River in Gujiao and Loufan Counties in western Taiyuan City, more grids with high cropland area fraction were found near rivers compared to high altitude areas.

In 1916, the cropland in Fenhe River Valley Plain began to expand to the north until 1937. The proportion of grids with a cropland area fraction more than 30% increased to 37.31% (Figure 6g). Moreover, the proportion of grids with a cropland area fraction more than 70% also peaked at 14.51% in 1937. Compared with the Qing Dynasty, although grids with high cropland fraction were also mainly concentrated in eastern Taiyuan City, the cropland fraction in northeastern Taiyuan City in the Republic of China was significantly higher than that of the Qing Dynasty. The cropland fraction in western Taiyuan City decreased after 1892, but a few grids with high cropland fraction were found in eastern Gujiao City, which was possibly because the eastern part of Gujiao City at present belonged to Yangqu County during 1916–1937.

In 1952, the cropland area declined in northern Fenhe River Valley Plain but increased in the southern part. The proportion of grids with cropland more than 70% decreased notably, dropping to 7.92% in 1952. These changes mainly occurred in the northern Fenhe River Valley Plain. Most grids with a cropland area fraction of more than 30% remained in eastern Taiyuan City. Moreover, the cropland expanded in southern Taiyuan City. The land in Qingxu County in southern Taiyuan City was extensively cultivated with an average cropland area fraction of 56.22% (Figure 6h).

In 1980, the rapid urbanization led to the conversion of cropland into construction land. The proportions of grids with cropland more than 30%, 50% and 70% are, respectively, 34.34%, 18.47% and 11.36%. The cropland area decreased sharply in the Fenhe River Valley Plain. Meanwhile, the high cultivated area shifted from the center of eastern Taiyuan City to the south and north. The cropland area fractions of Qingxu and Yangqu Counties in the northern and southern Taiyuan City all increased to 68.06% and 18.48% in 1980 (Figure 6i). The cropland area fraction of Gujiao City, west of Taiyuan City, also increased rapidly, from 10.81% in 1937 to 17.09% in 1980.

## 5. Discussions

### 5.1. Comparison with Satellite-Based Data

To validate our cropland gridded allocation model, we compare our cropland area in 1980 with the satellite-based cropland cover data with a resolution of 1 km × 1 km in the 1980s [61].

Due to the different methods of obtaining cropland data, the county-level cropland area from satellite-based cropland cover data in 1980s is higher than that from survey data (Figure 7). The county-level cropland area based on the satellite-based cropland cover map in 1980s is allocated to 1 km × 1 km grids using our cropland gridded allocation model. Then, we compare the allocated 1 km × 1 km cropland area data (Figure 8a) with the satellite-based 1 km × 1 km cropland cover data in the 1980s (Figure 8b). Their spatial distribution patterns of cropland area are close overall. Grids with high cropland area fraction are mainly distributed in northern and eastern Taiyuan City in two maps.

However, there are still some differences between them. The difference map is calculated by subtracting the 1 km resolution satellite-based cropland cover map from our spatial distribution map of cropland in 1980. A total of 95.77% of the grids have differences between −20% and +20%. Grids with differences of more than 40% are scattered in the northeastern and central parts of Taiyuan City. Grids with large differences are scattered in areas with less cropland (Figure 8c). The larger the difference, the smaller the number of grids (Table 4). In our reconstruction, the areas with more allocated cropland have a larger potential maximum spatial extent of cropland and relatively lower altitude, whereas the areas with less allocated cropland have a smaller potential maximum spatial extent of cropland and a higher altitude. This may indicate that our cropland gridded allocation

model has a slightly higher weighting of altitude and potential maximum spatial extent of cropland.

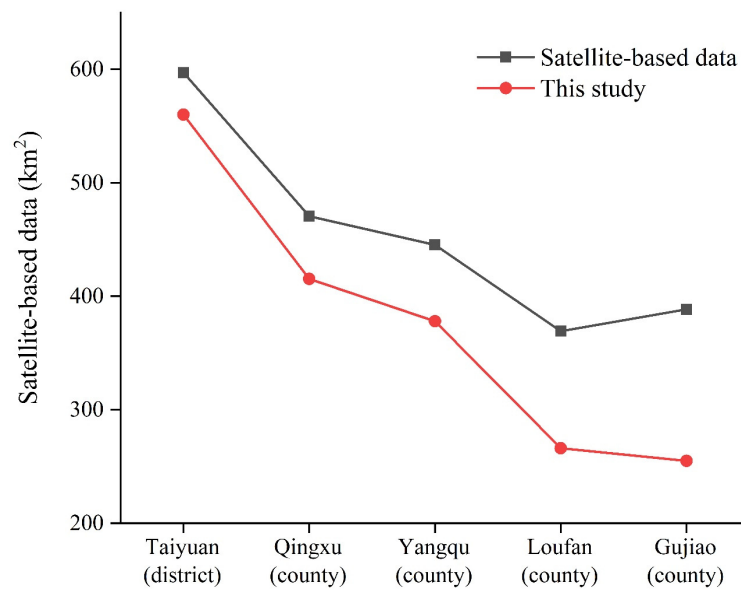


**Figure 7.** Comparison between the cropland areas in 1980 from satellite-based cropland cover data and this study.

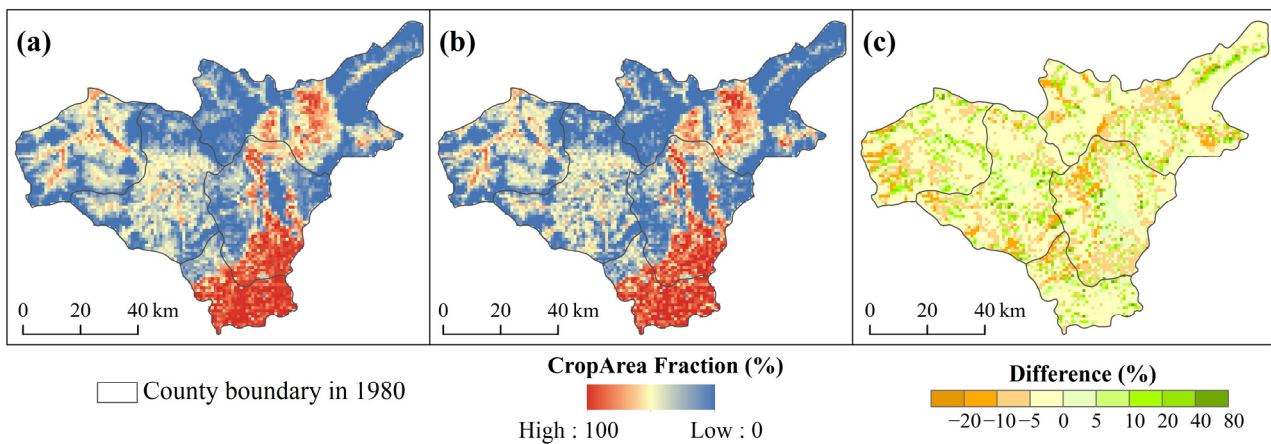


**Figure 8.** Comparison between our reconstruction and the satellite-based cropland cover data in 1980s: (a) the allocated cropland area; (b) satellite-based cropland cover data in 1980s; (c) differences between (a,b).

**Table 4.** Classification of differences between our allocated cropland area and the satellite-based cropland cover data in 1980s.

Differences (%)	[80~40)	[40~20)	[20~10)	[10~5)	[5~0)	[0~-5)	[-5~-10)	[-10~-20)	[-20~-40)
Percentage of grids (%)	0.71	3.38	5.35	4.57	8.55	54.33	17.79	5.19	0.14

### 5.2. Comparison with HYDE3.2 Dataset

There is still uncertainty when applying the global historical land use datasets at the regional scale, especially in cropland, which may lead to both underestimation and overestimation [31,32]. By comparing the History Database of the Global Environment

(version 3.2, HYDE3.2) [18] with our results, the accuracy of HYDE3.2 in Taiyuan City can be evaluated. The spatial resolution of HYDE3.2 dataset is 5', whereas the grid cell size of our results is 1 km. Therefore, our results are aggregated to 5', and the comparison is performed at the 5' scale (Figure 9).

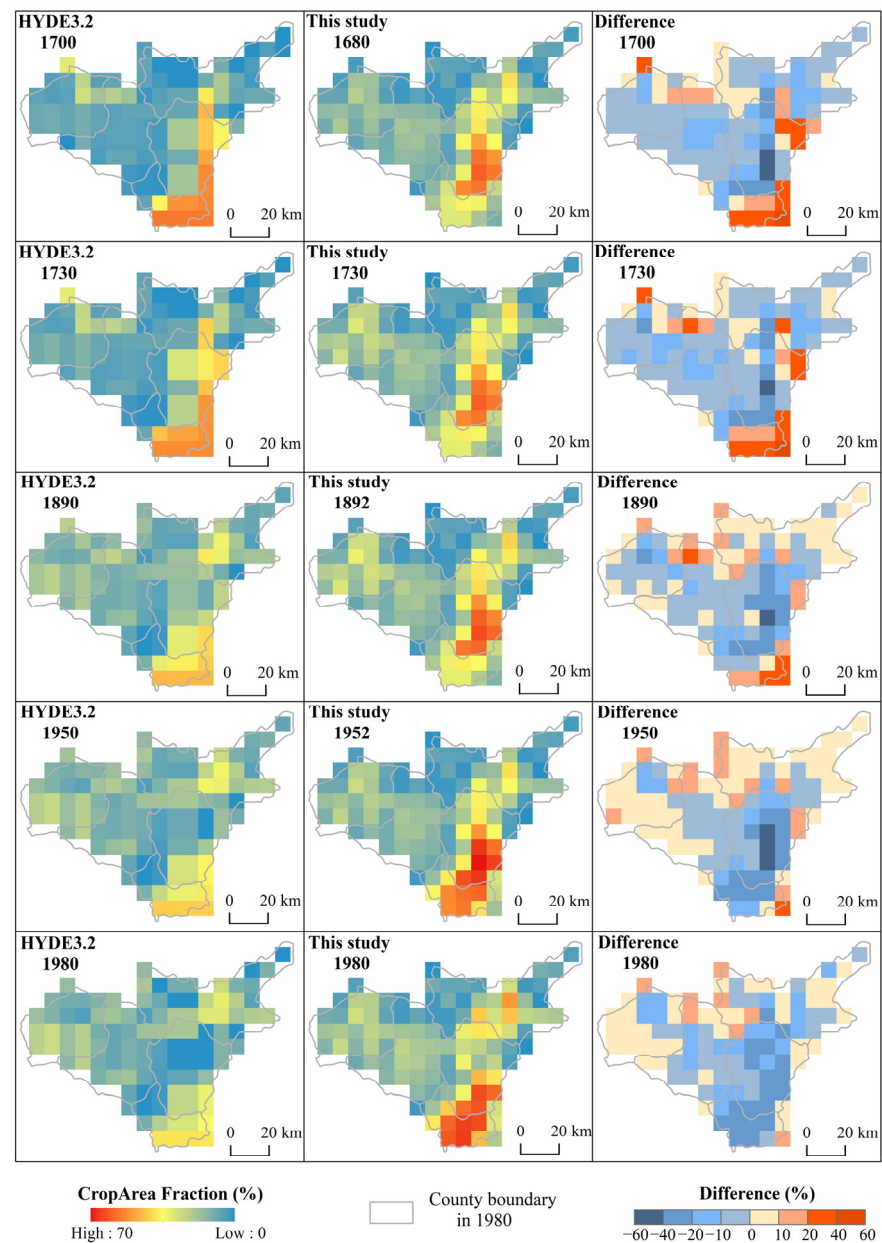


**Figure 9.** Comparisons between the HYDE3.2 dataset and our reconstruction results in 1700, 1730, 1892, 1952, and 1980.

The cropland area in this study is generally higher than that in the HYDE3.2 dataset. The data sources of the HYDE3.2 dataset are at the national and provincial level, and there is an absolute limit to obtain accurate county-level cropland area through the gridded allocation of national and provincial-level cropland area, but the data sources of this study are at the county level. Moreover, based on the two maps, we find that the spatial distribution patterns of cropland are close between the HYDE3.2 and our results. They show the most cropland in eastern Taiyuan City and less cropland in western Taiyuan City. However, differences can also be detected between the two datasets. We observe that in HYDE3.2, cropland was mainly distributed in southern and eastern Taiyuan City during

1700–1980. From 1700 to 1980, the cropland in these areas with a higher cropland area fraction decreased gradually. Meanwhile, the cropland in western Taiyuan City increased stably. In our results, we observe that cropland was mainly distributed in the Fenhe River Valley Plain from 1680 to 1892. The cropland in central and eastern Taiyuan City increased from 1680 to 1952, and it decreased in 1980. Moreover, the cropland in southern Taiyuan City increased rapidly from 1952 to 1980. In western Taiyuan City, the cropland area increased slightly from 1680 to 1892, then decreased in 1952, and increased in 1980.

Differences of most grids are between  $-10\%$  and  $+10\%$ . The proportion of grids with differences between  $-10\%$  and  $+10\%$  increased from 60.55% in 1700 to 64.22% in 1950, while it declined to 59.63% in 1980. Grids with higher differences (more than 20% and less than  $-20\%$ ) were mainly distributed in southern and eastern Taiyuan City, and differences of these areas gradually declined after 1950. By comparing the methods of reconstructing the spatial distribution of historical cropland between our results and HYDE3.2, the possible reason for the differences is using cropland area in different levels. HYDE3.2 uses continental or national-level cropland areas and only can show historical cropland changes in large-scale regions, while we use county-level cropland areas. Therefore, the cropland allocation method of HYDE3.2 does not consider the differences among counties in Taiyuan City. For example, in our results, the cropland areas of counties with good economic conditions like Yangqu and Taiyuan Counties were more than in HYDE3.2 from 1700 to 1980. With worse economic conditions, the cropland areas of Qingxu County in southern Taiyuan were less than HYDE3.2 from 1700 to 1890 and then increased to more than HYDE3.2 after 1950. These may cause the differences between our results and the HYDE3.2.

### 5.3. Uncertainties

This study effectively improved the accuracy of gridded allocation by using historical county-level cropland area, but this method also caused discontinuity in the spatial patterns of cropland at county boundaries. The cropland gridded allocation model also has some limitations:

Firstly, our model relies too heavily on land suitability as indicated by physiogeographic factors and ignores the abandonment of cropland due to sudden environmental changes or human activities during the historical period. We use the modern cropland fraction to correct for land suitability, which may result in the preferential allocation of cropland to grids with saturated cropland in modern.

Secondly, according to Wu et al. [37,38], a grid with higher land suitability for cultivation need not be planted with crops first. Therefore, they devise a new method for cropland gridded allocation that uses settlements to denote the location and chronological sequence of human cultivation activities. However, due to the absence of the data of settlements in Taiyuan City, we ignore the factor of settlements in establishing a cropland gridded allocation model. Moreover, our cropland gridded allocation model does not involve the impact of historical construction land change on the spatial patterns of cropland. In the future, the reconstruction of historical cropland changes in provincial capital cities, the factors of construction land change and settlements will be added into our gridded allocation model.

## 6. Conclusions

In this study, historical documents, survey data, and statistics are collected to reconstruct the cropland area of each county in Taiyuan City from 1650 to 1980. We construct a cropland gridded allocation model for Taiyuan City and allocate the cropland area to grids with a resolution of  $1\text{ km} \times 1\text{ km}$ . We also validate the accuracy of our results and compare them with the HYDE3.2 dataset. Our reconstruction could enhance the accuracy of the global dataset and serve as base data in studying historical climate change. The major conclusions are as follows.

The changes trend of total cropland area from 1650 to 1980 can be divided into four stages. From 1650 to 1784, the total cropland area in Taiyuan consistently increased. Then, the cropland area decreased slightly from 1784 to 1892. After that, it increased rapidly from 1892 to 1937. Finally, the total cropland area declined sharply from 1937 to 1952, and it increased after 1952.

The cropland spatial distribution patterns show that cropland was mainly distributed in the Fenhe River Valley Plain from 1650 to 1892. Cropland expanded to the northern Taiyuan City after 1916 and gradually increased until 1937. Subsequently, land cultivation in southern Taiyuan City greatly intensified from 1952 to 1980. The cropland area in central Taiyuan City decreased rapidly in 1980.

The accuracy of our reconstruction has been validated by comparing with the satellite-based cropland cover data in 1980s, despite the total cropland area of each county being smaller than that from satellite-based cropland cover data. The comparison of cropland spatial distribution patterns exhibits substantial similarity between them. Most of the cropland is distributed in northern and eastern Taiyuan City. The HYDE3.2 dataset is lower than our reconstruction, especially in eastern and southern Taiyuan City.

**Author Contributions:** M.L.: Conceptualization, Methodology, Writing; X.W.: Conceptualization, Writing—review and editing; B.L.: Reviewing and Editing. All authors have read and agreed to the published version of the manuscript.

**Funding:** This research was funded by the National Natural Science Foundation of China (grant No.41807433, grant No.41972193 and grant No.42101103).

**Data Availability Statement:** The data presented in this study are available on request from the corresponding author.

**Acknowledgments:** The authors thank the anonymous reviewers for the helpful comments that improved this manuscript.

**Conflicts of Interest:** The authors declare no conflict of interest.

## References

1. GLP. *Science Plan and Implementation Strategy*; IGBP Report No. 53/IHDP Report No. 19; IGBP Secretariat: Stockholm, Sweden, 2005; p. 64.
2. Pongratz, J.; Raddatz, T.; Reick, C.H.; Esch, M.; Claussen, M. Radiative forcing from anthropogenic land cover change since A.D. 800. *Geophys. Res. Lett.* **2009**, *36*, L02709. [[CrossRef](#)]
3. Sterling, S.M.; Ducharne, A.; Polcher, J. The impact of global land-cover change on the terrestrial water cycle. *Nat. Clim. Chang.* **2012**, *3*, 385–390. [[CrossRef](#)]
4. Borrelli, P.; Robinson, D.A.; Fleischer, L.R.; Lugato, E.; Ballabio, C.; Alewell, C.; Meusburger, K.; Modugno, S.; Schutt, B.; Ferro, V.; et al. An assessment of the global impact of 21st century land use change on soil erosion. *Nat. Commun.* **2017**, *8*, 2013. [[CrossRef](#)] [[PubMed](#)]
5. Friedlingstein, P.; O’Sullivan, M.; Jones, M.W.; Andrew, R.M.; Gregor, L.; Hauck, J.; Le Quéré, C.; Luijkx, I.T.; Olsen, A.; Peters, G.P.; et al. Global Carbon Budget 2022. *Earth Syst. Sci. Data* **2022**, *14*, 4811–4900. [[CrossRef](#)]
6. Jia, G.; Shevliakova, E.; Artaxo, P.; De Noblet-Ducoudré, N.; Houghton, R.; House, J.; Kitajima, K.; Lennard, C.; Popp, A.; Sirin, A.; et al. Land–climate interactions. In *Climate Chang. and Land: An IPCC Special Report on Climate Chang., Desertification, Land Degradation, Sustainable Land Management, Food Security, and Greenhouse Gas Fluxes in Terrestrial Ecosystems*; Bernier, P., Espinoza, J., Eds.; IPCC: Geneva, Switzerland, 2019; Volume 2, pp. 131–247.
7. Feddema, J.J.; Oleson, K.W.; Bonan, G.B.; Mearns, L.O.; Buja, L.E.; Meehl, G.A.; Washington, W.M. The importance of land-cover change in simulating future climates. *Science* **2005**, *310*, 1674–1678. [[CrossRef](#)] [[PubMed](#)]
8. Future Earth. *Future Earth Initial Design Report[R/OL]*; Future Earth: Montréal, QC, Canada, 2013.
9. Wu, S.H.; Zhao, Y.; Tang, Q.H.; Zheng, J.Y.; Gao, H.B.; Liang, T.; Ge, Q.S. Land surface pattern studies for the Future Earth program. *Prog. Geogr.* **2015**, *34*, 10–17. (In Chinese)
10. Lepers, E.; Lambin, E.; Janetos, A.; Defries, R.; Achard, F.; Ramankutty, N.; Robert, J.; Scholes, A. A synthesis of information on rapid land-cover change for the period 1981–2000. *BioScience* **2005**, *55*, 115–124. [[CrossRef](#)]
11. Bondeau, A.; Smith, P.; Zaehle, S. Modelling the role of agriculture for the 20th century global terrestrial carbon balance. *Glob. Chang. Biol.* **2007**, *13*, 679–706. [[CrossRef](#)]
12. Gaillard, M.J.; Morrison, K.; Madella, M.; Whitehouse, N. Past land-use and land-cover change: The challenge of quantification at the subcontinental to global scales. *Past Land Use Land Cover* **2018**, *26*, 3.

13. Harrison, S.P.; Gaillard, M.-J.; Stocker, B.D.; Vander Linden, M.; Klein Goldewijk, K.; Boles, O.; Braconnot, P.; Dawson, A.; Fluet-Chouinard, E.; Kaplan, J.O.; et al. Development and testing scenarios for implementing land use and land cover changes during the Holocene in Earth system model experiments. *Geosci. Model Dev.* **2020**, *13*, 805–824. [[CrossRef](#)]
14. Goldewijk, K.K.; Battjes, J.J. *A Hundred Year (1890–1990) Database for Integrated Environmental Assessments (HYDE, version 1.1)*; Report No. 422514002; National Institute of Public Health and the Environment: Bilthoven, The Netherlands, 1997.
15. Goldewijk, K.K. Estimating global land use change over the past 300 years: The HYDE Database. *Glob. Biogeochem. Cycles* **2001**, *15*, 417–433. [[CrossRef](#)]
16. Goldewijk, K.K. The HYDE 3.1 spatially explicit database of human-induced global land-use change over the past 12,000 years. *Glob. Ecol. Biogeogr.* **2011**, *20*, 73–86. [[CrossRef](#)]
17. Goldewijk, K.K.; Beusen, A.; Doelman, J.; Stehfest, E. Anthropogenic land use estimates for the Holocene–HYDE 3.2. *Earth Syst. Sci. Data* **2017**, *9*, 927–953. [[CrossRef](#)]
18. Ramankutty, N.; Foley, J.A. Estimating historical changes in global land cover: Croplands from 1700 to 1992. *Glob. Biogeochem. Cycles* **1999**, *13*, 997–1027. [[CrossRef](#)]
19. Pongratz, J.; Reick, C.; Raddatz, T.; Claussen, M. A reconstruction of global agricultural areas and land cover for the last millennium. *Glob. Biogeochem. Cycles* **2008**, *22*, GB3018.1–GB3018.16. [[CrossRef](#)]
20. Kaplan, J.O.; Krumhardt, K.M.; Zimmermann, N. The prehistoric and preindustrial deforestation of Europe. *Quat. Sci. Rev.* **2009**, *28*, 3016–3034. [[CrossRef](#)]
21. Kaplan, J.O.; Krumhardt, K.M.; Ellis, E.C.; Ruddiman, W.F.; Lemmen, C.; Goldewijk, K.K. Holocene carbon emissions as a result of anthropogenic land cover change. *Holocene* **2010**, *21*, 775–791. [[CrossRef](#)]
22. Hurtt, G.C.; Chini, L.P.; Frolking, S.; Betts, R.A.; Feddema, J.; Fischer, G.; Fisk, J.P.; Hibbard, K.; Houghton, R.A.; Janetos, A.; et al. Harmonization of land-use scenarios for the period 1500–2100: 600 years of global gridded annual land-use transitions, wood harvest, and resulting secondary lands. *Clim. Chang.* **2011**, *109*, 117–161. [[CrossRef](#)]
23. Hurtt, G.C.; Chini, L.; Sahajpal, R.; Frolking, S.; Bodirsky, B.L.; Calvin, K.; Doelman, J.C.; Fisk, J.; Fujimori, S.; Klein Goldewijk, K.; et al. Harmonization of global land use change and management for the period 850–2100 (LUH2) for CMIP6. *Geosci. Model Dev.* **2020**, *13*, 5425–5464. [[CrossRef](#)]
24. Cao, B.; Yu, L.; Li, X.; Chen, M.; Li, X.; Hao, P.; Gong, P. A 1 km global cropland dataset from 10 000 BCE to 2100 CE. *Earth Syst. Sci. Data* **2021**, *13*, 5403–5421. [[CrossRef](#)]
25. Skaloš, J.; Weber, M.; Lipský, Z.; Trpáková, I.; Šantrůčková, M.; Uhlířová, L.; Kukla, P. Using old military survey maps and orthophotograph maps to analyse long-term land cover changes—Case study (Czech Republic). *Appl. Geogr.* **2011**, *31*, 426–438. [[CrossRef](#)]
26. Tian, H.; Banger, K.; Bo, T.; Dadhwal, V.K. History of land use in India during 1880–2010: Large-scale land transformations reconstructed from satellite data and historical archives. *Glob. Planet. Chang.* **2014**, *121*, 78–88. [[CrossRef](#)]
27. Yu, Z.; Lu, C. Historical cropland expansion and abandonment in the continental U.S. during 1850 to 2016. *Glob. Ecol. Biogeogr.* **2017**, *27*, 322–333. [[CrossRef](#)]
28. Paudel, B.; Zhang, Y.; Li, S.; Liu, L. Spatiotemporal changes in agricultural land cover in Nepal over the last 100 years. *J. Geogr. Sci.* **2018**, *28*, 1519–1537. [[CrossRef](#)]
29. He, F.; Yang, F.; Zhao, C.; Li, S.; Li, M. Spatially explicit reconstruction of cropland cover for China over the past millennium. *Sci. China Earth Sci.* **2023**, *66*, 111–128. [[CrossRef](#)]
30. He, F.N.; Li, S.C.; Zhang, X.Z.; Ge, Q.S.; Dai, J.H. Comparisons of cropland area from multiple datasets over the past 300 years in the traditional cultivated region of China. *J. Geogr. Sci.* **2013**, *23*, 978–990. [[CrossRef](#)]
31. Yu, L.; Wang, J.; Li, X.; Li, C.; Zhao, Y.; Gong, P. A multi-resolution global land cover dataset through multisource data aggregation. *Sci. China Earth Sci.* **2014**, *57*, 2317–2329. [[CrossRef](#)]
32. Fang, X.; Zhao, W.; Zhang, C.; Zhang, D.; Wei, X.; Qiu, W.; Ye, Y. Methodology for credibility assessment of historical global LUCC datasets. *Sci. China Earth Sci.* **2020**, *63*, 1013–1025. [[CrossRef](#)]
33. Gaillard, M.J.; LandCover6k Interim Steering Group Members. LandCover6k: Global anthropogenic land-cover change and its role in past climate. *Past. Glob. Chang. Mag.* **2015**, *23*, 38–39. [[CrossRef](#)]
34. Yang, X.; Jin, X.; Guo, B.; Long, Y.; Zhou, Y. Research on reconstructing spatial distribution of historical cropland over 300 years in traditional cultivated regions of China. *Glob. Planet. Chang.* **2015**, *128*, 90–102. [[CrossRef](#)]
35. Li, S.; He, F.; Zhang, X. A spatially explicit reconstruction of cropland cover in China from 1661 to 1996. *Reg. Environ. Chang.* **2015**, *16*, 417–428. [[CrossRef](#)]
36. Ye, Y.; Fang, X.; Ren, Y.; Zhang, X.; Chen, L. Cropland cover change in Northeast China during the past 300 years. *Sci. China Ser. D Earth Sci.* **2009**, *52*, 1172–1182. [[CrossRef](#)]
37. Wu, Z.; Fang, X.; Jia, D.; Zhao, W. Reconstruction of cropland cover using historical literature and settlement relics in farming areas of Shangjing Dao during the Liao Dynasty, China, around 1100 AD. *Holocene* **2020**, *30*, 1516–1527. [[CrossRef](#)]
38. Wu, Z.; Fang, X.; Ye, Y. A Settlement Density Based Allocation Method for Historical Cropland Cover: A Case Study of Jilin Province, China. *Land* **2022**, *11*, 1374. [[CrossRef](#)]
39. Wei, X.; Ye, Y.; Zhang, Q.; Li, B.; Wei, Z. Reconstruction of cropland change in North China Plain Area over the past 300 years. *Glob. Planet. Chang.* **2019**, *176*, 60–70. [[CrossRef](#)]

40. Li, Y.; Ye, Y.; Zhang, C.; Li, J.; Fang, X. A spatially explicit reconstruction of cropland based on expansion of polders in the Dongting Plain in China during 1750–1985. *Reg. Environ. Chang.* **2019**, *19*, 2507–2519. [[CrossRef](#)]
41. Huo, R.L.; Yang, Y.D.; Man, Z.M. Gridded reconstruction of the spatial and temporal evolution of cropland in Zhangjiu River Basin in mountainous Yunnan, 1700–1978. *Acta Geogr. Sin.* **2020**, *75*, 1966–1982. (In Chinese)
42. Wang, Q.; Xiong, M.; Li, Q.; Li, H.; Lan, T.; Deng, O.; Huang, R.; Zeng, M.; Gao, X. Spatially Explicit Reconstruction of Cropland Using the Random Forest: A Case Study of the Tuojiang River Basin, China from 1911 to 2010. *Land* **2021**, *10*, 1338. [[CrossRef](#)]
43. Wang, F.; Ye, Y.; Zhang, C.; Fang, X. Reconstruction of cropland cover using historical literature in Northern China, Sui Dynasty, AD 609. *Holocene* **2023**, *33*, 310–320. [[CrossRef](#)]
44. Zhang, C.; Fang, X.; Ye, Y.; Tang, C.; Wu, Z.; Zheng, X.; Zhang, D.; Jiang, C.; Li, J.; Li, Y.; et al. A spatially explicit reconstruction of cropland cover in China around 1850 C.E. employing new land suitability based gridded allocation algorithm. *Quat. Int.* **2022**, *641*, 62–73. [[CrossRef](#)]
45. Local Gazetteers Compilation Committee of Taiyuan City. *The Chronicles of Taiyuan*; Shanxi Ancient Books Press: Taiyuan, China, 1990.
46. Xia, R.B.; Wang, W. Rice planting in Shaanxi during the Ming and Qing Dynasties. *J. Chin. Hist. Geogr.* **2020**, *35*, 72–82. (In Chinese)
47. Zhang, H.Z. *The Relation between the Economic and the Environmental in Fenhe River Basin in the Ming and Qing Dynasty*; Shaanxi Normal University Press: Xi'an, China, 2005.
48. Fu, L.X.; Lin, J.; Ren, Y.X.; Wang, W.D. *A General History of Administrative Districts in China—Qing Dynasty Volume*, 2nd ed.; Fudan University Press: Shanghai, China, 2017.
49. Fu, L.X.; Zheng, B.H. *A General History of Administrative Districts in China—Republic of China*, 2nd ed.; Fudan University Press: Shanghai, China, 2017.
50. Beijing Astronomical Observatories Chinese Academy of Sciences. *A General Catalogue of Gazetteers in China*; China Book Council: Beijing, China, 1985.
51. Phoenix Press. *Collection of Chinese Gazetteers Shanxi Province*; Phoenix Press: Nanjing, China, 2005.
52. Buck, J.K. *Land Utilization in China—Statistics*; The Commercial Press: Beijing, China, 1937.
53. Statistics Section, General Affairs Department, Ministry of Agriculture and Commerce. *Fifth Agriculture and Commercial Statistics Table in the Fifth Year of the Republic of China*; Shanghai China Book Council: Shanghai, China, 1919.
54. Shanxi Provincial Department of Agricultural Construction and Bureau of Statistics Press. *Compilation of Statistics on Agriculture, Forestry and Water Resources in Shanxi Province, Prewar-1956 Volume 1*; Shanxi Provincial Department of Agricultural Construction and Bureau of Statistics Press: Taiyuan, China, 1957.
55. National Bureau of Statistics. *Summary of Rural Economic Statistics by County in China (1980–1987)*; China Statistics Press: Beijing, China, 1989.
56. Committee for Integrated Survey of Natural Resources in the Chinese Academy of Sciences and State Planning Commission. *Datasets of Land and Resources of China*; Committee for Integrated Survey of Natural Resources in the Chinese Academy of Sciences and State Planning Commission, Chinese Academy of Sciences: Beijing, China, 1989.
57. Cao, S.J. *History of Chinese Population*; Fudan University Press: Shanghai, China, 2001; Volume 5.
58. Hou, Y.F. *History of Chinese Population*; Fudan University Press: Shanghai, China, 2001; Volume 6.
59. Duan, M.; Tian, Q. *Compilation of Demographic Historical Materials of the Republic of China*; National Library Press: Beijing, China, 2009.
60. Xu, X.L. *Spatial Distribution Dataset of Annual Vegetation Index (NDVI) in China*; Resource Environmental Science Data Registry and Publishing System: Beijing, China, 2018.
61. Xu, X.L.; Liu, J.Y.; Zhang, S.W.; Li, R.D.; Yan, C.Z.; Wu, S.X. *Multi-Period Land Use Remote Sensing Monitoring Dataset in China*; Resource Environmental Science Data Registry and Publishing System: Beijing, China, 2018.
62. He, B.K. *Examination and Evaluation of Ancient and Modern Land in China*; China Social Science Press: Beijing, China, 1988.
63. Zhang, Q.Y. *A Study of Land Use and Driving Factors in Northern Jin during the Qing Dynasty*; Shaanxi Normal University Press: Xi'an, China, 2012.
64. Ge, Q.S.; Dai, J.H.; He, F.N.; Zheng, J.Y.; Man, Z.M.; Zhao, Y. Analysis of changes in the quantity of cropland resources and driving factors in some Chinese provinces and regions over the past 300 years. *Prog. Nat. Sci.* **2003**, *13*, 43–50. (In Chinese)
65. Wei, X.; Ye, Y.; Zhang, Q.; Fang, X. Methods for cropland reconstruction based on gazetteers in the Qing Dynasty (1644–1911): A case study in Zhili province, China. *Appl. Geogr.* **2015**, *65*, 82–92. [[CrossRef](#)]
66. Wang, J.F.; Xu, C.D. GeoDetector: Principles and Prospects. *Acta Geogr. Sin.* **2017**, *72*, 116–134. (In Chinese)
67. Wei, G.; Liu, Y. The analysis of spatiotemporal evolution of economic and environmental coordination development degree in Liaoning coastal economic belt. *Acta Geogr. Sin.* **2012**, *31*, 2044–2054. (In Chinese)
68. Chang, Y.; Ji, X. Research on Evaluation and Driving Factors of Sustainable Development of Chinese Sub-Provincial Cities Based on Public Participation. *Open Access Libr. J.* **2020**, *7*, 1–13. [[CrossRef](#)]
69. Li, F.B. Land reclamation in direct Shanxi in the early Qing dynasty. *Chin. Hist. Geogr. Ser.* **1995**, *3*, 71–78. (In Chinese)
70. Shanxi Agricultural Zoning Commission. *Modern Agricultural Economy of Shanxi*; Agricultural Press: Beijing, China, 1990.
71. Li, F.B. An Essay on the Reclamation of Traditional Agricultural Areas in the Direct Shanxi Province during the Middle and Late Qing Dynasty. *Chin. Hist. Geogr. Ser.* **1994**, *2*, 147–162. (In Chinese)
72. Xu, W.Y. *History of Economic Development of Shanxi*; Shanxi Economic Press: Taiyuan, China, 1993.

73. Zhang, W.G. Destruction of agroforestry ecosystems in Shanxi during the war period. *J. Shanxi Social. Acad.* **2017**, *2*, 73–77. (In Chinese)
74. Liu, X.; Jing, Z.K. *Financial and Economic History of the Jinsui Border Region*; Shanxi Economic Press: Taiyuan, China, 1993.
75. Department of Rural Socio-Economic Surveys, National Statistical Office. *Compilation of Agricultural Statistics in China (1949–2004)*; China Statistics Press: Beijing, China, 2006.

**Disclaimer/Publisher’s Note:** The statements, opinions and data contained in all publications are solely those of the individual author(s) and contributor(s) and not of MDPI and/or the editor(s). MDPI and/or the editor(s) disclaim responsibility for any injury to people or property resulting from any ideas, methods, instructions or products referred to in the content.